ARTICLE

# Biocompatible Graft Copolymers from Bacterial Poly(γ-Glutamic Acid) and Poly(Lactic Acid)

Received 00th January 20xx,
Accepted 00th January 20xx

DOI: 10.1039/x0xx00000x

Cristiana L. Zaccaria,[a] Valeria Cedrati,[a] Andrea Nitti,[a] Enrica Chiesa,[b] Antxon Martinez de Ilarduya,[c] Monserrat Garcia-Alvarez,[c] Massimiliano Meli,[d] Giorgio Colombo,[a,d] Dario Pasini*[a]

We report on a novel approach to the modular and convergent construction of biocompatible graft copolymers starting from bacterial poly(γ-glutamic acid)(γ–PGA) and incorporating poly(lactic acid) (PLA). The synthetic strategy is controlled at different levels: a) the choice of a suitable initiator for the ring-opening polymerization of lactide; b) the chemical elaboration of the polylactic fragments; c) their convergent "grafting to" functionalization of bacterial γ-PGA propargyl ester using copper(I)-catalyzed alkyne-azide cycloaddition (CuAAC) click chemistry. The graft copolymers are characterized in terms of their thermal and macromolecular properties, their conformational preferences through molecular modelling, and their cytotoxicity.

## Introduction

Poly(γ-glutamic acid) (γ-PGA),[1] formally a nylon 4 derivative, is a bacterial polymer used in the cosmetic and food industries. It is obtained from renewable resources (by fermentation, from a series of bacteria strains),[2-4] and its characteristics are excellent as a macromolecular backbone for innovative biomaterials. The scientific interest around γ-PGA has greatly risen in the last 20 years.[5-9]

The α-carboxylic group of γ-PGA can be derivatized, to modulate the physical and chemical properties of the native biopolymer.[10] Several strategies for γ-PGA functionalization have been recently proposed.[11-14] We have recently reported a remarkably efficient alkylation methodology using homogeneous reaction conditions in low polarity organic solvents. Solubilization of γ-PGA is obtained by exchanging the cation associated to the carboxylate functionalities with a long alkyl chain quaternary ammonium cation. Esterified γ-PGA homo or copolymers, containing allyl or propargyl groups, have been obtained in high yields. CuAAC click chemistry[15] have then been used, in the case of propargyl esters, to install further functional groups onto the γ-PGA backbone.[16]

Block copolymers, which can be simplified as the covalent merging of different types of macromolecules, have been widely explored, for improving the properties of the separate polymeric components, and for providing interesting and property-directed conformations and morphologies, with recent outstanding examples in the field of nanoscience and nanopatterning.[17] In the context of biomaterials, block copolymers are common, but graft copolymers have not been as widely explored to date. Examples of graft copolymers have been reported as a potential strategy for enhancing biostability properties,[18] or enhancing drug delivery performance.[19] Even considering one of the most popular biocompatible scaffolds, poly(lactic acid) (PLA), it is perhaps surprising to find only a few reports on its incorporation in graft copolymers: these reports are mainly based on the polymerization of preformed methacrylate PLA macromonomers.[20,21]

The synthetic difficulties in addressing the reliable and controlled functionalization of γ-PGA have hampered a modular and molecularly precise approach to γ-PGA based graft copolymers. In the few reports available, γ-PGA based graft copolymers are built with unoptimal control of the degree of functionalization and of the coverage of the pendant chains from the main γ-PGA backbone.[22,23]

Here we report about the synthesis, characterization, and properties of a new family of graft copolymers in which biocompatible polyesters are efficiently "clicked" onto the γ-PGA backbones. The overall synthetic strategy is schematically illustrated in Figure 1. The modularity of the synthesis takes advantage of the controlled ring-opening polymerization (ROP) of lactide, so that the initiating functionality is effectively inserted at one chain end. The other chain end is chemically elaborated, with a simple, innovative protocol, to introduce the azide reactive terminal functionality, which is then clicked onto propargyl-functionalized γ-PGA ester. The modularity of the synthetic approach allowed us to systematically change the PLA length grafted onto the main backbone, uncovering interesting thermal properties of the graft copolymers. Structural characterization through conformational search techniques provides initial atomic-resolution insight into the structural preferences of model copolymers. Citotoxicity tests demonstrated the preeminent role of the initiating ROP

[a] Department of Chemistry and INSTM Research Unit, University of Pavia, Via Taramelli 10 –27100 Pavia – Italy. Email: dario.pasini@unipv.it
[b] Department of Civil Engineering and Architecture, University of Pavia, Via Ferrata 3 –27100 Pavia – Italy.
[c] Departament d'Enginyeria Química, Universitat Politècnica de Catalunya, ETSEIB, Diagonal 647 – 08028 Barcelona – Spain.
[d] SCITEC-CNR, Via Mario Bianco 9 – 20131 Milano – Italy.

Electronic Supplementary Information (ESI) available: Additional graphs figures and tables, copies of NMR spectra of new polymers presented in the paper. See DOI: 10.1039/x0xx00000x

functionality, which decorate the exterior of the graft copolymer, in determining the toxicity of the final graft copolymer.

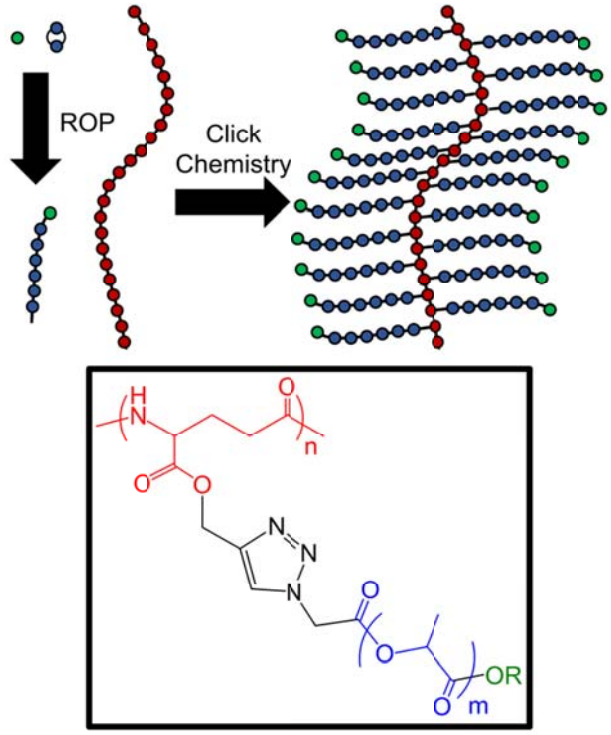


**Figure 1.** A schematic view of the modular synthetic approach to PLA-grafted γ-PGA copolymers, and the chemical structure of the synthesized copolymers (bottom).

## Results and Discussion

**Synthesis of the γ-PGA graft copolymers.** The convergent synthesis of the graft polymers is achieved in five overall steps, starting from the cyclic dimer of lactic acid (lactide) on one side and γ-PGA on the other side. Poly(lactic acid) (PLA) was chosen as polyester scaffold because it is amongst the most studied biocompatible polyesters. Its green nature, mostly afforded by the fact that the monomer is produced by fermentation, and then polymerized,[24] makes it extremely appealing in combination with γ-PGA. Its relatively low cost makes it very competitive and currently used in the field of bioplastics. PLA can be obtained through a ROP approach, in which the use of a specific alcohol initiator allows for the precise positioning of the initiating residue as one of the end chain functionalities. Once clicked convergently onto the γ-PGA scaffold, as described in Figure 1, such initiating functionalities will fully decorate the whole comb-like macromolecules, and therefore could have a decisive impact in controlling the overall properties of the macromolecular construct. The initial preparation of the PLA precursors is reported in Scheme 1. *LL*-lactide (lactide is the cyclic dimer of lactic acid) was used consistently for all the experiments reported below. Several methodologies, already present in the literature, were initially tested by us for the ROP of lactide. When compared to either diazabicycloundecene (DBU) or tin octanoate ($Sn(Oct)_2$) as the catalysts, better results were obtained in our hands using 4-dimethylaminopyridine (DMAP) as the catalyst.[25] The use of the DMAP, an organocatalyst, in the ROP possesses obvious advantages, in terms of the overall sustainability of the synthetic process, and for avoiding contamination of the final product with potentially toxic tin-based catalysts. In our optimized protocol DMAP was used in substoichiometric quantities in dry $CH_2Cl_2$ as solvent and gentle heating for 24 h. Polymers **4** were obtained with benzylic alcohol **1** (Scheme 1) as the initiator in essentially quantitative yields as waxes after purification by precipitation in hexanes. Good agreement between the observed and calculated ratio of monomers could be observed by $^1H$ NMR, by the relative integration of the unique proton resonances of the initiating residue and of the repeating units and values were confirmed by GPC measurements. As reported in the literature,[25] we were able to confirm the controlled nature of the ROP polymerization. The linear relationships between conversion and number average $M_n$, the first order nature of the kinetics, and the narrow resulting dispersities are shown in Figure S1. By using ethanol **2** as the initiator, polymer **5a** was obtained in a similarly controlled manner, and it was brought throughout the functionalization sequence shown in Scheme 1.

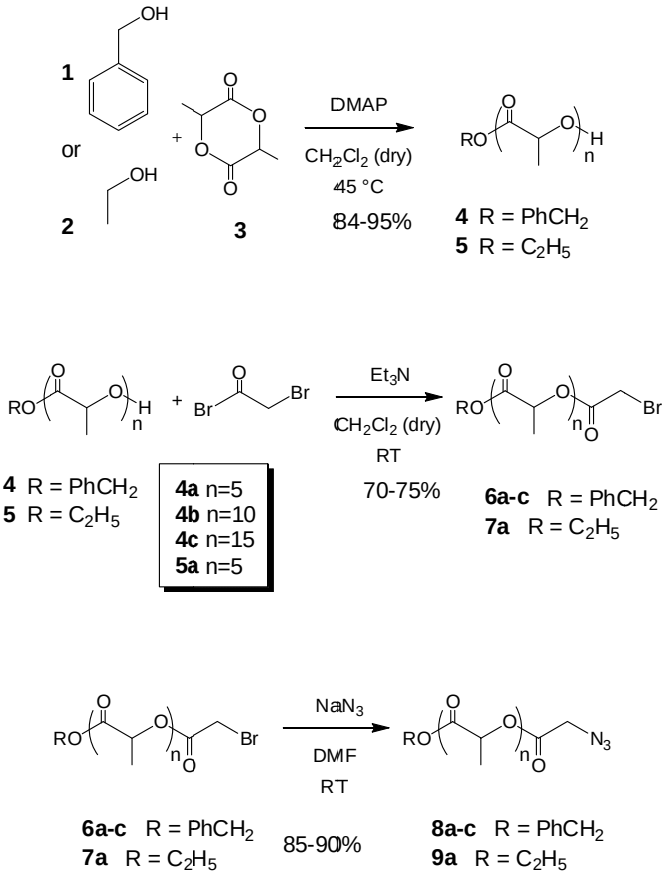


**Scheme 1.** Synthesis of PLA through ROP, and subsequent chemical elaboration for the insertion of the azide terminal units.

To our knowledge, the only known derivatization of PLA to introduce a terminal azide involves a two step procedure, consisting in the transformation of the terminal secondary alcohol into a good leaving group (methanesulfonate) and subsequently a substitution reaction on the secondary carbon using sodium azide.[26] This procedure could not be reproduced reliably in our hands. We

therefore successfully designed another two step procedure, which has the advantage of transforming the terminal secondary alcohol of the PLA chains in a primary terminal alkyl bromide, prone to be transformed into the azide by a straightforward substitution reaction (Scheme 1). The acylation reaction was conducted with bromoacetyl bromide in the presence of triethylamine, to obtain derivatives **6** and **7** in good yields. The substitution of bromine with an azido-terminal group takes place at room temperature with an excess of $NaN_3$ (1.5 equivalent) and DMF as a solvent. Polymers **8** and **9** could be obtained in pure form after precipitation in hexane as the nonsolvent.

Propargyl functionalized γ-PGA **10** was obtained as a copolymer, with a high degree of esterification, as described in our previous paper.[16] The lack of complete esterification in the case of γ-PGA is a consequence of steric factors;[16] several batches of polymer **10** showed consistently and reliably a substitution coverage of propargyl groups of around 90%, as indicated in Scheme 2. Polymer **10** was reacted with azido and benzyl terminated PLA polymers **8a-c** (used in slight excess). The reaction conditions for the click chemistry ($CuSO_4$/Na ascorbate in a mixed DMF/$H_2O$ solvent system) were previously optimized on model systems, and afforded fully functionalized graft copolymers **12a-c** in excellent yields in all cases. Polymers **12** were carefully purified by precipitation in acidic water, and then a second purification by dissolving the crude in THF and reprecipitating it in hexane. The fidelity of the convergent, "grafting onto" approach using the optimized CuAAC protocol was verified by NMR spectroscopy (see below). The protocol was equally successful using ethyl ester terminated azido PLA **9a**, to afford polymer **13a** in good yields.

In order to verify the efficiency and the reliability of our convergent functionalization strategy, we made an experiment in which PLA **8c** was used in less than stoichiometric quantities (ca. 0.5 equivalents). Indeed, terpolymer **11c**, in which ca. 50% of alkyne terminal functionalities were still prone to further functionalization, was obtained in good yields using the previously mentioned CuAAC protocol. Polymer **13c** could be further functionalized (Scheme 2) with compound **14** to obtain fully "clicked" polymer **15c** in high yields. All polymers could be obtained as white powders, after thorough purification procedures involving at least two purification into nonsolvents.

**FTIR, NMR, GPC and Thermal Characterization of the Graft Copolymers.**

Infrared spectra of **12a-c** and **15c** graft copolymers are depicted in Figure S2. These spectra display two weak peaks at 1654 $cm^{-1}$ and 1542 $cm^{-1}$ corresponding to the stretching and bending vibrations of amide carbonyl and N-H functional groups, respectively. A strong absorption peak could be detected at 1750 $cm^{-1}$ and corresponds to the stretching vibration of ester carbonyl group of PLA side chains. As it can be observed, the intensity of this peak increases with the length of the PLA side chain. NMR spectroscopy was essential to confirm the structure and to determine the composition of the graft copolymers. The $^1H$ NMR ($CDCl_3$) spectra of representative samples for polymers **6-9** are shown in Figure 2 with attributions, and highlight how the transformation of the endchain functional groups occurs quantitatively. The inset highlights the unexpected small changes in the resonances of the terminal $CH_2$ units (ca. 3.91 ppm in polymer **6a** and **7a** to 3.96 ppm in polymer **8a** and **9a**) upon the transformation of the terminal bromide into azide. Further confirmation of the complete transformation to azide came from the IR spectrum, which shows the distinctive absorption peak at 2110 $cm^{-1}$, corresponding to the stretching of the -$N_3$ group.

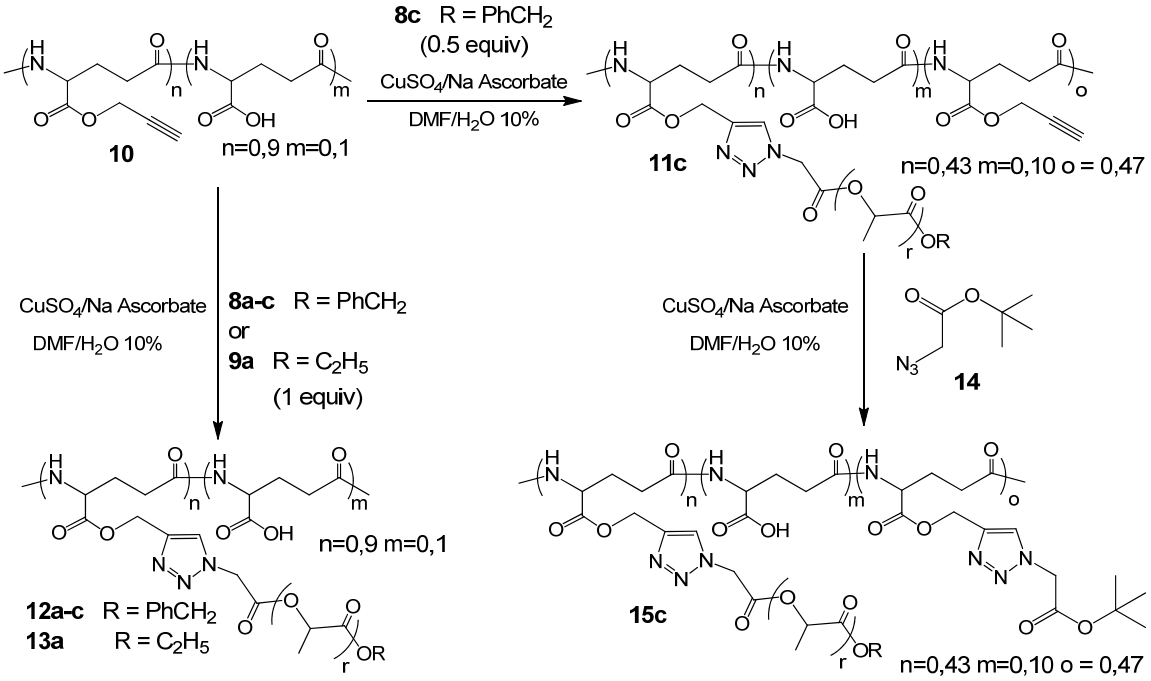


**Scheme 2.** Synthesis of graft γ-PGA PLA copolymers. Estimated copolymer composition determined by NMR spectroscopy of the purified products.

ARTICLE

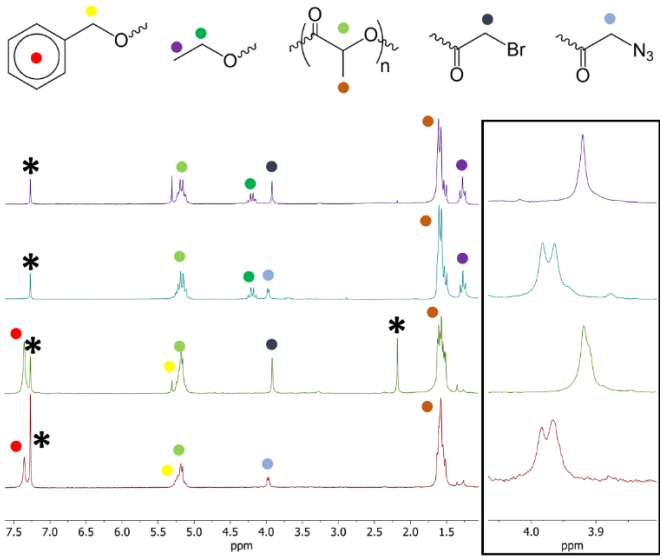


**Figure 2.** Comparison of the $^{1}$H NMR spectra ($CDCl_3$) of polymers (from bottom to top: **8a**, **6a**, **9a**, **7a**). Inset: enlargement of the full NMR spectra on the left showing the -$COCH_2$-X terminal units at ca. 4 ppm. The asterisks indicate solvent impurities.

$^{1}$H NMR and $^{13}$C NMR spectra of polymers **11c**, **12a-c**, **13a** and **15c** confirmed the efficiency of the click coupling and of the purification procedures. Better resolution and reduced broadening of the signals was achieved at 80°C in deuterated DMSO.

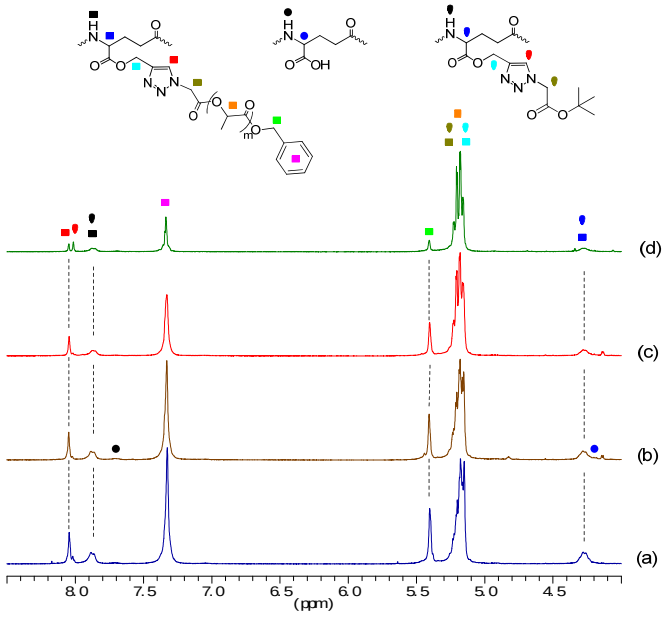


**Figure 3.** $^{1}$H-NMR spectra of (a) polymer **12a**, (b) polymer **12b**, (c) polymer **12c** with increasing length of PLA side chains and (d) polymer **15c**.

As an example, the 4-9 ppm region of graft copolymers is shown in Figure 3 (full spectra are depicted in the SI). NH proton signals of functionalized (at ca. 7.9 ppm) and unfunctionalized (at ca. 7.7 ppm) portions of the copolymers are distinguishable.

The disappearance of the $^{1}$H NMR spectra of the unique signals of the propargyl ester groups (for example, the proton resonances of the $CH_2C{\equiv}C$ groups at ca. 4.7 ppm), and from the appearance of the newly formed aromatic triazole proton resonances at ca. 8.1 ppm confirmed the efficiency of the CuAAC click synthetic protocol. Two signals in this region were observed for polymer **15c**, due to the double functionality of the side chains (PLA and *tert*-butyloxy carbonyl) built on γ-PGA. The absence of any residual signal related to the $COCH_2N_3$ terminal units of the PLA reagent at ca. 4 ppm, together with the coherence of the proton resonance integrations with the proposed structure, confirmed that any excess or unreacted PLA chains had been efficiently removed.

Important information was also gathered from the $^{13}$C NMR spectroscopy (Figure S3). In the region of around 170 ppm, both carbonyls of ester and amide groups of the γ-PGA units can be observed at 171.5 and 171.4 ppm respectively. On the other hand, carbonyls of PLA units can be observed in the range 169.1-169.4 ppm. As the length of PLA side chain increases, the signals due to inner carbonyls, which can be observed at 169.1 ppm, increases in intensity over outer carbonyls which appear at 166.6 and 169.4 ppm. These signals are not split, confirming that no racemization of the *L*-lactic acid units took place, both during the ring opening polymerization, as well as during the click reaction.

The thermal stability of graft copolymers were evaluated by termogravimetric analysis carried out under inert atmosphere (Figure 4 and Figure S4). Grafted γ-PGA with increased length of PLA side chains (polymers **12a-c**) were stable up to around 270 ºC. The remaining weight at 600ºC decreased with the content of these units in the copolymer (Table S1). It is likely that unzipping transesterification reactions of lactate units with generation of volatile *LL*-lactide could be responsible for this thermal behavior. For polymer **15c**, the slight weight loss at around 180ºC is attributable to the presence of the thermally labile *tert*-butoxycarbonyl groups, with a good match between the calculated (loss of isobutylene, on the basis of the structure and the copolymer composition determined by $^{1}$H NMR) and observed (3.4% calcd vs. 2.4% observed) weight loss starting at 160 °C and ending at 200 ºC.

DSC heating traces (second heating scan) of polymers **12a-c** and **15c** showed second order transitions, attributed to the glass transition temperatures, and remarkably in line with literature values for PLA samples.[27] Additionally, broad endotherms at 118 and 108 ºC were observed for polymers **15c** and **12c** respectively in the first heating DSC thermograms (Figure S5), which we attributed to the melting of crystals made of short PLA grafted chains. These peaks were not observed for polymers **12** with shorter PLA side chains. It is very

interesting to note that the thermal properties of the graft copolymers are essentially dominated by the PLA pendant chains, and that the insertion of the PLA chains of suitable length (polymers **12b** and **12c**) was able to profoundly modify the thermal behavior of γ-PGA, since glass transitions for the graft macromolecular constructs can be observed. It must be reminded that γ-PGA by itself does not show any glass or melting transition temperatures, but instead decomposes upon heating around 200°C through an unzipping depolymerization mechanism with release of pyroglutamic acid.[28]

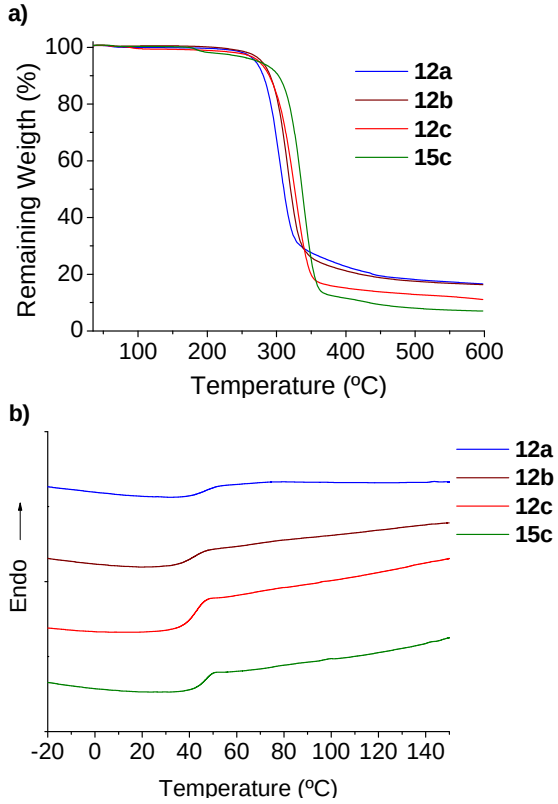


**Figure 4.** (a) TGA and (b) DSC traces (second heating scan) of PLA graft γ-PGA copolymers.

Powder X-ray diffraction measurements were performed for PLA grafted samples **12a-c** and **15c**. As it can be observed in Figure 5, sample **12c** displayed representative diffraction peaks at 2 theta Bragg angles of 14.8, 16.7, 19.0, 22.3 corresponding to the (010), (110/200), (203), (204) planes, respectively, attributed to PLA side chains crystallized in the α-crystalline form.[29,30,31] To calculate the phase crystalline content, crystalline peaks were extracted from the diffraction pattern by peak deconvolution and a crystalline index of 17 % was estimated for this sample (Figure S6). These diffractions were not detected in sample **12a** and scarcely observed in sample **12b** indicating that the length of the PLA side chain plays a key role in this crystallization. On the other hand sample **15c** displayed a diffraction pattern similar to sample **12b** although a broad melting peak at 118 °C is observed by DSC. This discrepancy could be attributed to a broad cold crystallization that could happen between the glass transition and melting during the heating process.

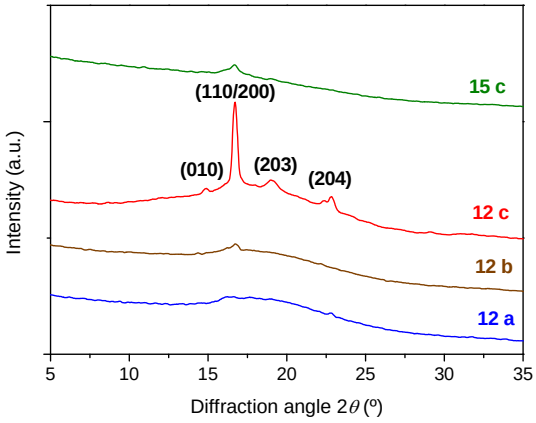


**Figure 5.** Powder WAXS profiles of PLA graft γ-PGA copolymers **12a-c** and **15c**.

Selected graft copolymers were characterized by GPC chromatography using dimethylacetamide (DMAc) as the solvent (see example in Figure S7), which solubilized well all the samples. The results are reported in Table 1. As previously reported, the reaction conditions used for synthesis brought a substantial reduction in the molecular weight from the bacterial γ-PGA starting polymer to propargyl functionalized γ-PGA **10**. Further functionalization by clicking did bring further reductions but the degree of polymerization in either **12b** or **15c** remained high. The *Đ* values remained remarkably similar during the whole synthetic process. Uncertainties in the GPC measurements may be severely enhanced by the compact, globular nature of the graft copolymers (see below molecular modelling), as opposed to the random coil conformations of the PMMA samples used as standards.

**Table 1.** Molecular weight characteristics of selected synthesized copolymers obtained by GPC in DMAc.[a]

| Polymer | $M_n$ | *Đ* | DP[b] |
|---|---|---|---|
| **10** | 121000 | 1,8 | 630 |
| **12b** | 188000 | 1,5 | 280 |
| **15c** | 182000 | 1,7 | 420 |

[a] For analysis method, see experimental part. *Đ* = dispersity index. [b] Degree of polymerization; calculated on the basis of $M_n$ values, using the weighted (according to composition determined by $^1$H NMR spectroscopy) average repeating unit molecular weight.

**Molecular Modelling and AFM studies.** The conformational preferences of the constituting units can be a key determinant of the supramolecular organizational behavior, propensity to further modification and interaction properties of the γ-PGA-based copolymers. To start shedding light on the conformational behavior of the triazole-lactic acid containing derivatives, we first studied a simplified system containing one unit of lactic acid and one unit of glutamate (namely *n, m* = 1). Towards this end, we used the Monte Carlo Molecular Mechanics (MCMM) conformational search method, as implemented in the Maestro Suite

(www.schrodinger.com), employing as variables all rotatable bonds, to sample the potential energy surface of the molecule in an octanol solvent model able to recapitulate typical laboratory conditions (octanol, organic solvent). The ensembles of sampled conformations were first subjected to cluster analysis, using an agglomerative method, to identify the most representative conformations. The structures representative of the most populated clusters are compact, with a tendency to form intramolecular hydrogen bonding interactions and to expose hydrophobic groups to contact with the solvent. Next, we set out to characterize the conformational preferences of a longer copolymer (*n= 1, m* = 5, Figure 6).

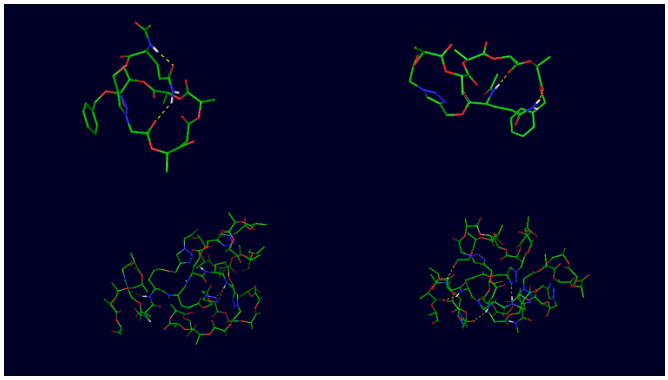

**Figure 6.** The structures of the 2 most populated clusters obtained from MD simulations for the PLA-PGA copolymers. The dotted lines represent intramolecular hydrogen bonding interactions. Top row: n=1, m=5. Bottom row: n = 5, m = 5.

Considering the length of the molecule, here we turned to Molecular Dynamics simulations to sample the conformational landscape. Simulations were once more run in octanol. The trajectories were analyzed by means of cluster analysis and time evolution of the radius of gyration (Figure S8). The copolymer populates compact conformations, whereby 2 main clusters are able to recapitulate most of the conformational diversity. It can be noticed, in particular, that one face of the triazole ring is shielded from the solvent by the folding on top of it of the lactate units. Finally, we set out to simulate a more extended system, with *n, m = 5* (Figure 6). In this system, the two most populated clusters show that the polymer tends to fold up in compact structures characterized by a core containing the triazole rings, in some cases engaged in intramolecular hydrogen bonding interactions with the amidic hydrogens, and an outside layer containing PLA repetitive units.

The folding behaviour indicated by the modelling studies suggest that these graft copolymers do not phase separate in terms of nanoscale morphology, since the two different blocks constituting the macromolecular structure (the polyglutamate and the polylactic units) are in fact hidden by each other in closed structures. Phase separation is instead common in well defined block copolymers.[32] AFM studies were therefore carried out in order to obtain information about the nanoscale morphology, phase systems and possible phase separations in thin films of copolymers **12a-c**. The observed morphologies in all the three films analyzed showed the absence of phase separation on the nanoscale, and confirmed the presence of essentially uniform films (Figure S9).

**Cytotoxicity Tests and Hydrophilicity Studies.** In order to establish the biocompatibility of the synthesized graft copolymers, 3-(4,5-dimehyilthiazol-2-yl)-2,5-diphenyltetrazolium bromide (MTT) assays were undertaken for selected samples (**12a** and **13a**) at the concentration range of 10 – 250 mg/mL.[33] As can be noted from Figure 7, raw γ-PGA does not show any evidence of cytotoxicity: the cell survival percentage is always higher than the relative blank control. Moreover, the highest γ-PGA concentrations (50 – 100 – 250 mg/mL) seem to promote cell viability along the first 24h of incubation confirming the well-known biocompatibility of the raw polymer.[2] As benchmark values, chitosan and hyaluronic acid, two frequently used polymers recognized as GRAS (Generally Recognized as Safe), show in MTT assays toxicity effects only at concentrations higher than 1 mg/mL.[34]

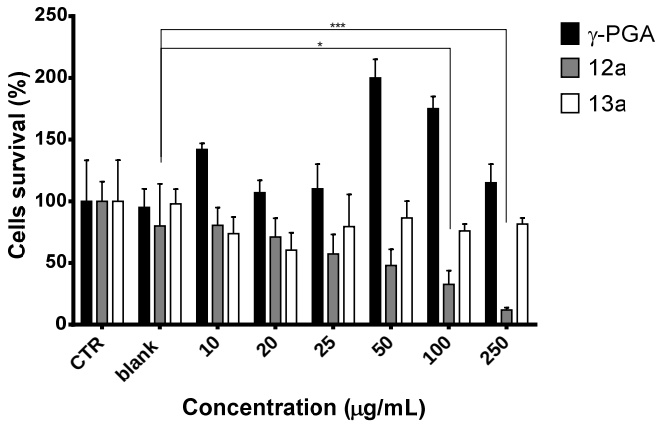


**Figure 7**. MTT assay performed on γ-PGA, **12a** and **13a** incubated for 24 h with Normal Human Dermal Fibroblast (NHDFs). The data represents the mean ± SD (n= 3 independent experiments). Results are expressed as cell survival percentage compared to the untreated cells (CTR). Blank is the negative control (solvent without polymers). Statistical differences for p value < 0.05 (*), p value < 0.001 (***).

Results concerning the benzyl terminated graft copolymer (**12a**), show a significant reduction of cellular survival if compared to the related blank control. The cytotoxicity effect of **12a** is concentration-dependent: the cell survival percentage decreases from 80 ± 14% to 11 ± 2% by increasing the polymer concentration. Statistical analysis (Dunnett's multiple comparisons test) reveals significant differences at 100 and 250 mg/mL compared to the blank counterpart. It is also evident that polymer **12a** triggers a notable reduction (p value < 0.05) of the γ-PGA biocompatibility at all the concentrations tested, and therefore we can speculate that toxicity was due to the use of benzyl alcohol as initiator.

Cytotoxicity data collected for polymer **13a**, presenting ethyl terminal functionalities, showed cell survival values always higher than 80% after 24h of incubation. This means that ethyl termination is able to improve the biocompatibility of benzyl terminated graft

copolymer. It is found to be a safe material that could be used in the biomedical field in the range of concentration 10–250 μg/mL.

Hydrophilicity studies were carried out by means of contact angle measurements on films cast and annealed in the polymer series **12a-c**. It was found that contact angle values with water were, respectively, 85.7°, 85.5°, 82.9° for **12a-c.** The result suggests a stable hydrophilicity of the films in the presence of increasing lengths of the hydrophobic PLA segments.

## Conclusions

We have reported a novel approach to the modular construction of biocompatible graft copolymers starting from bacterial γ-PGA and PLA. The synthetic strategy takes advantage of a convergent approach. The ROP of lactide using either benzyl or ethyl alcohol as the initiator is followed by the innovative postfunctionalization approach of the PLA terminal ends, to introduce an azide. We demonstrated the efficiency and precision of the CuAAC click chemistry for the coupling of the azido-terminated PLA chains onto the propargyl terminated γ-PGA, to afford a family of graft copolymers in which the PLA chain lengths were systematically varied.

The conformational preferences through molecular modelling indicated a globular, compact structure for the graft copolymers. AFM studies confirmed the absence of phase-separated morphologies in thin films of the graft copolymers, built from two very different monomeric units. Their thermal properties indicate a profound effect of the introduction of the PLA pendant chains, since glass thermal transitions could be observed. In the derivatives with longer PLA grafted chains, there are evidences that the PLA side chains are able to crystallize in the α crystalline form. When ethyl ester functionalities decorate the exterior of the macromolecules, cytotoxicity is brought to values comparable to those of currently used polymers and biopolymers in the biomaterials arena.

Considering that γ-PGA by itself does not show any glass or melting transition temperatures, the described approach may open up possibilities in the 3D printing and/or bulk processing of such macromolecular constructs.

## Experimental Section

***General Experimental.*** γ-PGA was purchased and characterized as previously described.[16] Compounds **10**[16] and **14**[35] were prepared as previously described. *LL*-Lactide was recrystallized from toluene before use. All other commercially available compounds were used as received. $^{1}$H and $^{13}$C NMR spectra were recorded from solutions in $CDCl_3$ or dimethyl sulfoxide (DMSO)-$d_6$ on 200, 300 or 400 MHz instruments and calibrated with the solvent residual proton signal. Infrared spectra were recorded on a FTIR spectrophotometer equipped with a diffuse reflectance accessory using KBr powder as the inert support.

Static contact angle determinations were made with a KSV CAM200 instrument, with the water sessile drop method. Samples were prepared by dissolving 30 mg of polymer in 1 mL of $CHCl_3$, then casting the solution onto a glass substrate. The resulting thin films were annealed at 80 °C for 24 hours, after which the oven was turned off and allowed to cool slowly to room temperature.

WASX diffraction patterns were recorded on the PANalytical X'Pert PRO MPD θ/θ diffractometer using the Cu Kα radiation of wavelength 0.1542 nm from powdered samples sandwiched between amorphous polyester films of 3.6 micron thicknesses.

***Gel permeation chromatography (GPC).*** For PLA samples GPC was carried out on a Waters system equipped with a RI detector. Samples were prefiltered using 0.4 μm Nylon or PTFE filters and then directly injected. The mobile phase was THF stabilized with BHT (2,6-di-*tert*-butyl-4-methylphenol) (1 mL/min, 40˚C) a set of two universal columns (Styragel 4E and 5E) in series. Low polydispersity polystyrene standards were used for the calibration curve (Fluka kit). Molecular weight distribution data ($M_w$, $M_n$ and dispersity) are obtained through elaboration with the software Breeze. For γ-PGA derivatives, GPC in DMAc was performed using two universal columns, thermostated at 30°C, and calibrated against PMMA standards.

***Computational Analysis.*** The conformational analyses and Molecular Dynamics (MD) simulations were conducted using the Maestro Suite of Programs from Schrodinger (www.schrodinger.com). The OLPS3[36] force field with the octanol solvent model was used in all phases of modeling.[37] The torsional conformational search for the compound with *n,m = 1* with 62 was carried out using the MCMM method[38,39] and a maximum number of steps were 30000. The non-bonded cut-offs were set to 8 Å for Van der Waals and 20A for the electrostatic interactions. Each new conformation found by the conformational search were minimized for 2500 steps of conjugate gradient method before the novelty check.[40] The most populated conformations were identified by the k-means clustering method, using the RMSD among conformations as a metrics for distances. MD simulations in implicit solvent water and octanol for the compounds with n = 1, m = 5 (98 atoms) and n = 5, m = 5 (387 atoms) were started from a completely extended conformation. The simulations start with a conjugate gradient minimization until the threshold of 0.05 [kcal mol$^{-1}$ Å$^{-1}$] on energy gradient is reached. The equilibration of 1 ns and the production phase of 300ns for the each system were carried out at 300K with an integration step of 1.5 fs. The SHAKE algorithm[41] was used to constrain bond lengths to their original values. The analysis on the trajectories and the conformational search were conducted by GROMACS analysis tools [www.gromacs.org].

***AFM analysis.*** All of the films were imaged using a Thermomicroscope AutoProbe CP Research II Atomic Force Microscope in tapping-mode with silicon cantilevers with resonance frequencies of about 160 kHz, spring constants of 5.0 N/m, and radii less than 10 nm. Samples were prepared by dissolving 30 mg of polymer in 1 mL of $CHCl_3$, then spin coating the solution onto a glass substrate at 1500 rpm for 60 s. The resulting thin films were annealed at 80 °C for 24 hours, after which the oven was turned off and allowed to cool slowly to room temperature.

***MTT assay.*** NHDFs were cultured in DMEM (Dulbecco's Modified Eagle Medium) supplied with 10% (v/v) Fetal Bovine Serum (FBS) and 1% (v/v) penicillin/streptomycin solution. Cells were trypsinized when subconfluent, seeded in a 96-well plate (seeding density= 10,000 cells/well) and incubated at 37° C in a 5% $CO_2$ for 24h till

reaching 70% of cell confluence. Cytotoxicity tests were performed by incubating NHDFs for 24 h at 37°C in a 5% $CO_2$ atmosphere with γ-PGA, **12a** and **13a** solutions at the concentration range of 10-250 mg/mL. Briefly, the selected compounds (γ-PGA, **12a** and **13a**) were dissolved in DMSO at different concentrations, namely 0.8, 1.6, 2, 4, 8 and 20 mg/mL. 50 μl of each solution was diluted with DMEM supplied with 10% (v/v) FBS and 1% (v/v) penicillin/streptomycin solution to reach a final concentration of 10, 20, 25, 50, 100, 250 mg/mL. 50 μl of DMSO diluted with DMEM was used as blank. An aliquot of 200 mL of each solution was incubated with cells for 24 h at 37°C in a 5% $CO_2$ atmosphere. Untreated cells were used as control (CTR). MTT assay evaluated the cells viability after incubation and results were expressed as viability percentage compared to untreated cells.

**Representative procedure for the synthesis of polymers 4 and 5 through ROP of lactide. Polymer 4a.** *Initiator-Lactide monomer ratio 1:2.5.* In an oven-dried flask, under $N_2$ atmosphere, *LL*-lactide (5.0 g, 34.7 mmol) and DMAP (3.4 g, 27.8 mmol) were dissolved in dry $CH_2Cl_2$ (60 mL). Benzyl alcohol **1** (1.5 g, 13.9 mmol) was then added. The reaction mixture was heated with stirring at 45°C for 24 h. The reaction mixture was washed with $H_2O$ (50 mL) and diluted HCl (0.1 N, 50 mL). The reaction solvent was removed *in vacuo*, the crude reaction was dissolved in a minimum amount of $CH_2Cl_2$ and the product purified by precipitation in hexane (200 mL). The precipitate was cooled to 4 °C for several hours, and then filtered and dried, to give polymer **4a** as a waxy white solid (6.1 g, 94%). $^1$H NMR ($CDCl_3$, 200 MHz) δ = 7.34 (bs, 5H, aromatics), 5.25-5.14 (m, 2H + ~5H, -$CH_2$- benzylic and –C<u>H</u>($CH_3$)- lactic polymer chain), 4.42-4.32 (q, 1H, -C<u>H</u>($CH_3$)-OH terminal unit), 3.79 (bs, 1H, -OH terminal), 1.60-1.42 (bm, ~15H, -$CH_3$ polymer chain). **Polymer 5a.** *Initiator-Lactide monomer ratio 1:2.5.* From *LL*-lactide (4.0 g, 28 mmol), DMAP (2.7 g, 22 mmol) and EtOH (0.65 mL, 11 mmol). Polymer **5a** was obtained as a waxy white solid (4.0 g, 85%). $^1$H NMR ($CDCl_3$, 200 MHz) δ = 5.25-5.06 (bs, 5H, -CH- polymer chain), 4.42-4.32 (bs, 1H, -C<u>H</u>OH terminal), 4.24-4.13 (bm, 2H, -$CH_2$- ethyl), 1.59-1.47 (bm, ca. 15H, -$CH_3$ polymer chain), 1.29-1.23 (bm, 3H, -$CH_3$ ethyl terminal).

**Representative procedure for the synthesis of polymers 6 and 7. Polymer 6a.** Polymer **4a** (1.0 g, 2.14 mmol of terminal functionalities) and $Et_3N$ (0.6 mL, 4.27 mmol) were dissolved in dry $CH_2Cl_2$ (10 mL). Bromoacetyl bromide (0.74 mL, 8.5 mmol) in dry $CH_2Cl_2$ (5 mL) was added dropwise at 0 °C. The reaction mixture was stirred at room temperature for 24 h, and then washed with $H_2O$ (3 x 15 mL), diluted HCl (0.1 M, 15 mL), $Na_2CO_3$ (1%, 15 mL) and again $H_2O$ (15 mL). The organic phase was dried ($Na_2SO_4$), filtered and the solvent removed *in vacuo* to give polymer **6a** as a waxy brown solid (0.9 g, 72%). $^1$H NMR ($CDCl_3$, 200 MHz) δ = 7.36 (bs, 5H, aromatics), 5.24-5.16 (m, 2H + ~5H, -$CH_2$- benzylic and –C<u>H</u>($CH_3$)- polymer chain), 3.92 (bs, 2H, terminal –$CH_2$Br), 1.63-1.51 (bm, ~15H, -CH(C<u>H</u>$_3$)- polymer chain). $^{13}$C NMR ($CDCl_3$, 75 MHz) δ = 169.4 (m, CO lactic), 166.5 (CO terminal), 135.0 ($C_{quat}$ Ar), 128.5-128.2 (CH Ar), 69.2 (m, CH lactic), 67.1 ($CH_2$Ph), 25.1 ($CH_2$Br), 16.5 (m, $CH_3$ lactic). **Polymer 7a.** From polymer **5a** (1.5 g, 3.7 mmol terminal functionalities), $Et_3N$ (0.87 mL, 6.28 mmol) and bromoacetyl bromide (1.1 mL, 13 mmol). Polymer **7a** was obtained as a waxy brown solid (1.4 g, 74%). $^1$H NMR ($CDCl_3$, 200 MHz) δ = 5.31-5.12 (bs, 1H, -CH- polymer chain), 4.25-4.15 (bs, 2H, -$CH_2$- ethyl), 3.92 (bm, 2H, -$CH_2$Br terminal), 1.61-1.5 (bm, ca. 15H, -$CH_3$ polymer chain), 1-31-1.24 (bm, 3H, -$CH_3$ ethyl).

**Representative procedure for the synthesis of polymers 8. Polymer 8a.** Polymer **6a** (1.0 g, 1.7 mmol of terminal chains) was dissolved in DMF (6 mL). Sodium azide ($NaN_3$) (0.17 g, 2.6 mmol) was added and the reaction mixture was stirred at room temperature for 24 h. The reaction was then partitioned by adding $NH_4Cl$ 1 M (8 mL) and $CH_2Cl_2$ as the organic phase (3 x 8 mL). The organic phase was washed once again with $NH_4Cl$ 1 M (3 x 6 mL), dried ($Na_2SO_4$) and filtered. The polymer was further purified by dissolving it in a minimum amount of $CH_2Cl_2$ and precipitation in hexane (200 mL). The precipitate was cooled to 4 °C for several hours, and then filtered and dried, to give polymer **8a** as a waxy solid (0.9 g, 91%). $^1$H NMR ($CDCl_3$, 200 MHz) δ = 7.36 (bs, 5H, <u>H</u> aromatics), 5.23-5.16 (m, 2H + ~5H,-C<u>H</u>$_2$- benzylic and –C<u>H</u>($CH_3$)- polymer chain), 3.98-3.97 (d, 2H, -C<u>H</u>$_2$$N_3$ terminal), 1.63-1.51 (bm, ~15H, -CH(C<u>H</u>$_3$)- polymer chain). $^{13}$C NMR ($CDCl_3$, 75 MHz) δ = 169.5-169.4 (m, CO lactic), 167.7 (CO terminal), 135.0 ($C_{quat}$ Ar), 128.5-128.1 (CH Ar), 69.4-68.9 (m, CH lactic), 67.1 ($CH_2$Ph), 49.9 ($CH_2N_3$), 16.6-16.5 (m, $CH_3$ lactic). IR ($cm^{-1}$) = 2108 ($N_3$ stretching), 1760, 1680, 1460. **Polymer 9a.** From polymer **7a** (1.2 g, 2.3 mmol), $NaN_3$ (0.21 g, 3.3 mmol), to give polymer **9a** as a waxy solid (1.1 g, 90%). $^1$H NMR ($CDCl_3$, 200 MHz) δ = 5.25-5.11 (bs, 5H, -C<u>H</u>- polymer chain), 4.25-4.14 (bs, 2H, -C<u>H</u>$_2$- ethyl), 3.98-3.96 (bm, 2H, -C<u>H</u>$_2$$N_3$ terminal), 1.6-1.49 (bm, ca. 15H, -C<u>H</u>$_3$ polymer chain), 1.3-1.24 (bm, 3H, -C<u>H</u>$_3$ ethyl terminal).

**Representative procedure for the click chemistry grafting and the synthesis of polymers 11c, 12a-c, 13a and 15c. Polymer 11c.** Polymer **10** (260 mg, 1.5 mmol) and polymer **8c** (1.4 g, 0.08 mmol of terminal functionalities) were dissolved in DMF (30 mL). $CuSO_4 \times 5H_2O$ (60 mg, 0.3 mmol) and sodium ascorbate (150 mg, 0.6 mmol) are added as catalyst. $H_2O$ (3 mL, 10% v/v) was slowly added to the solution, and the reaction mixture was stirred at room temperature for 24 h. The polymer is purified by precipitation in a solution of diluted HCl (0.1 M, 800 mL), filtered and dried. It was further redissolved in a small amount of $CH_2Cl_2$ and precipitated in hexane (500 mL), filtered and dried, to afford polymer **11c** as a white powder (850 mg, 51%). $^1$H NMR ($CD_3SOCD_3$, 200 MHz) δ = 8.31 (bs, 1H; NH), 8.13 (bs, 1H; -C<u>H</u>- triazole), 7.35 (bs, 5H; H aromatic), 5.50 (bs, 2H; -NC<u>H</u>$_2$COO-), 5.17 (bm, 24H, -C<u>H</u>- PLA chain and -COOC<u>H</u>$_2$-), 4.70 (bs, 2H; -C<u>H</u>$_2$ propargyl $CH_2$), 4.21 (bs, 1H; -C<u>H</u>- γ-PGA chain), 3.50 (bs, 1H; terminal triple bond -C<u>H</u>), 2.21-1.76 (bm, 4H; -C<u>H</u>$_2$- γ-PGA chain), 1.47-1.44 (bm, 66H; -C<u>H</u>$_3$ PLA chain). **Polymer 12a.** From Polymer **10** (0.22 g, 1.3 mmol) and polymer **8a** (1.0 g, 1.82 mmol of terminal functionalities) to afford polymer **12a** as a white powder (1.0 g, 85%). $^1$H NMR ($CD_3SOCD_3$, 200 MHz) δ = 8.26-8.24 (bs, 1H, NH γ-PGA), 8.12 (bs, 1H, -CH- triazole), 7.34 (bs, 5H, aromatic), 5.5 (bs, 2H, -$NCH_2$- PLA chain), 5.2-5.14 (bm, 5H, -CH- PLA chain, 2H, -$COOCH_2$-) 4.26-4.18 (bs, 1H, -CH- γ-PGA chain), 2.23-1.76 (bm, 4H, -$CH_2$- γ-PGA chain), 1.46-1.12 (bm, ca. 15H, -$CH_3$ PLA). $^{13}$C NMR ($CDCl_3$, 100 MHz) δ = 172.2-172.0 (CO γ-PGA), 169.5-169.4 (m, CO lactic), 166.7 (CO terminal), 142.0 ($C_{quat}$ triazole), 135.0 ($C_{quat}$ Ar), 128.5-128.1 (CH Ar), 126.2 (CH triazole), 69.4-68.0 (m, CH lactic), 66.5 (<u>C</u>$H_2$Ph), 58.2 (COO<u>C</u>$H_2$ γ-PGA), 51.8 (α-<u>C</u>H γ-PGA), 50.0

(triazole-$\underline{C}H_2$), 31.0 ($\gamma$-$\underline{C}H_2$ $\gamma$-PGA), 26.5 ($\beta$-$\underline{C}H_2$ $\gamma$-PGA), 16.6-16.5 (m, $CH_3$ lactic). **Polymer 13a.** From polymer **10** (0.2 g, 1.16 mmol) and polymer **9a** (0.8 g, 1.62 mmol) to afford polymer **13a** as a white powder (870 mg, 87%). $^1$H NMR ($CD_3SOCD_3$, 200 MHz) $\delta$ = 8.13 (bs, 1H, N$\underline{H}$ $\gamma$-PGA), 7.94 (bs, 1H, -C$\underline{H}$- triazole), 5.5 (bs, 2H, -NC$\underline{H}_2$- PLA chain), 5.22-5.18 (bm, 5H, -C$\underline{H}$- PLA chain, 2H, -COOC$\underline{H}_2$-, 2H, -C$\underline{H}_2$- ethyl) 4.22-4.09 (bs, 1H, -C$\underline{H}$- $\gamma$-PGA chain), 2.23-1.76 (bm, 4H, -C$\underline{H}_2$- $\gamma$-PGA chain), 1.47-1.4 (bm, ca. 15H, -C$\underline{H}_3$ PLA), 1.21-1.14 (bm, 3H, -C$\underline{H}_3$ ethyl terminal). **Polymer 15c.** From polymer **11c** (124 mg, 0.07 mmol of terminal alkyne functionalities) and compound **14** (14 mg, 0.09 mmol), to afford polymer **15c** as a white powder (138 mg, quantitative). $^1$H NMR ($CD_3SOCD_3$, 200 MHz) $\delta$ = 8.26-8.24 (bs, 1H, NH $\gamma$-PGA), 8.12 (bs, 1H, -CH- triazole), 7.34 (bs, 5H, aromatics), 5.5 (bs, 2H, -NC$H_2$- PLA chain), 5.2-5.14 (bm, 5H, -CH- PLA chain, 2H, -COOC$H_2$-) 4.26-4.18 (bs, 1H, -CH- $\gamma$-PGA chain), 2.23-1.76 (bm, 4H, -C$H_2$- $\gamma$-PGA chain), 1.46-1.34 (bm, ca. 15H, -$CH_3$ PLA and *t*-butyl). $^{13}$C NMR ($CDCl_3$, 100 MHz) $\delta$ = 172.2-172.0 (CO $\gamma$-PGA), 169.5-169.4 (m, CO lactic), 166.7 (CO terminal), 142.0 ($C_{quat}$ triazole), 135.0 ($C_{quat}$ Ar), 128.5-128.1 (CH Ar), 126.2 (CH triazole), 82.0 ($\underline{C}(CH_3)_3$), 69.4-68.0 (m, CH lactic), 66.5 ($\underline{C}H_2Ph$), 58.2 (COO$\underline{C}H_2$ $\gamma$-PGA), 51.8 ($\alpha$-$\underline{C}H$ $\gamma$-PGA), 51.2-50.8 (triazole-$\underline{C}H_2$), 31.0 ($\gamma$-$\underline{C}H_2$ $\gamma$-PGA), 27.2 ($C(\underline{C}H_3)_3$), 26.5 ($\beta$-$\underline{C}H_2$ $\gamma$-PGA), 16.6-16.5 (m, $CH_3$ lactic).

## Author Contributions

D.P. designed the project, supervised C.L.Z., V.C. and A.N, and wrote the first draft of the paper. C.L.Z. and V.C. performed the experimental work, with substantial contributions by A.N. and E.C. A.M.D.I. and M.G.-A. performed characterization work. G.C. and M. M. performed the computational analysis. Results were discussed with the contributions of all authors. The manuscript was written through contributions of all authors.

## Conflicts of interest

There are no conflicts to declare.

## Acknowledgements

We thank Sebastian Munoz Guerra (UPC), Bice Conti and Ida Genta (University of Pavia) for useful discussion, Eugenio Roà and Aurora Pacini (UNIPV) for early involvement in this work, Maddalena Patrini (UNIPV) for the AFM studies, Lorenzo de Vita and Piersandro Pallavicini (UNIPV) for contact angle measurements, and Amitav Sanyal (Bogazici University, Turkey) for selected GPC experiments. The University of Pavia (postdoctoral fellowship type A to AN), INSTM (Consorzio Interuniversitario Nazionale per la Scienza e Tecnologia dei Materiali)-Regione Lombardia (Joint Call for Proposals, GAMMA-PGA Project, and PGGABIOMAT Project), Alma Mater Ticinensis Foundation (Excellence in Research, GAMMA-PGA Project) are gratefully acknowledged for financial support. A.M.D.I. and M.G.-A. acknowledge Ministerio de Ciencia e Innovación of Spain (MCIU/AEI/FEDER, UE) for the grant RTI2018-095041-B-C33.

## Notes and references

1 B. Rehm, *Nat. Rev. Microbiol.* 2010, **8**, 578–592.
2 J. M. Buescher and A. Margaritis, *Crit. Rev. Biotechnol.* 2007, *27*, 1–19.
3 V. Scoffone, D. Dondi, G. Biino, G. Borghese, D. Pasini, A. Galizzi and C. Calvio, *Biotechnol. Bioeng.* 2013, **110**, 2006–2012.
4 F. B. Oppermann, S. Fickaitz and A. Steinbüchel, *Polym. Degrad. Stabil.* 1998, **59**, 337–344.
5 I. Bajaj and R. Singhal, *Bioresour. Technol.* 2011, **102**, 5551–5561.
6 L. Zhang, X. Geng, J. Zhou, Y. Wang, H. L. Gao, Y. Zhou and J. Huang, *J. Drug Target.* 2015, **23**, 453–461.
7 S. Sakuma, T. Sagawa, Y. Masaoka, M. Kataoka, S. Yamashita, Y. Shirasaka, I. Tamai, Y. Ikumi, T. Kida and M. Akashi, *J. Control. Release* 2009, **133**, 125–131.
8 M. Matsusaki, T. Serizawa, A. Kishida and M. Akashi, *Biomacromolecules* 2005, **6**, 400–407.
9 D. Puppi, C. Migone, A. Morelli, C. Bartoli, M. Gazzarri, D. Pasini and F. Chiellini, *J. Bioact. Compat. Polym.* 2016, **31**, 531–549.
10 S. Muñoz-Guerra, M. García-Alvarez and J. A. Portilla-Arias, *J. Renew. Mater.* 2013, **1**, 42–60.
11 M. Morillo, A. Martínez de Ilarduya and S. Muñoz-Guerra, Polymer 2003, **44**, 7557–7564.
12 H. Kubota, Y. Nambu and T. Endo, J. *Polym. Sci. A Polym. Chem.* 1993, **31**, 2877–2878.
13 M. Biagiotti, G. Borghese, P. Francescato, C. F. Morelli, A. M. Albertini, T. Bavaro, D. Ubiali, R. Mendichi and G. Speranza, *RSC Adv.* 2016, **6**, 43954–43958.
14 A. Pacini, M. Caricato, S. Ferrari, D. Capsoni, A. Martínez de Ilarduya, S. Muñoz-Guerra and D. Pasini, J. *Polym. Sci. A. Polym. Chem.* 2012, **50**, 4790–4799.
15 L. Han, Q. Xie, J. Bao, G. Shan, Y. Bao and P. Pan, *Polym. Chem.* 2017, **8**, 1006–1016.
16 V. Cedrati, A. Pacini, A. Nitti, A. Martínez de Ilarduya, S. Muñoz-Guerra, A. Sanyal and D. Pasini, *Polym. Chem.* 2020, **11**, 5582–5589.
17 a) J. Bang, U. Jeong, R. Du Yeol, T. P. Russell and C. J. Hawker, *Adv. Mater.* 2009, **21**, 4769–4792. b) J. M. Klopp, D. Pasini, J. M. J. Frechet, C.G. Willson and J. D. Byers, *Chem. Mater.* 2001, **13**, 4147–4153.
18 K. Ishimoto, M. Arimoto, T. Okuda, S. Yamaguchi, Y. Aso, H. Ohara, S. Kobayashi, M. Ishii, K. Morita, H. Yamashita and N. Yabuchi, *Biomacromolecules* 2012, **13**, 3757−3768.
19 D. J. Price, M. Khuphe, R. P. W. Davies, J. R. McLaughlan, N. Ingram and P. D. Thornton, *Chem. Commun.* 2017, **53**, 8687−8690.
20 C. Juin, V. Langlois, P. Guerin and A. L. Borgne, *Macromol. Rapid Commun.* 1999, **20**, 289−293.
21 V. Langlois, K. Vallee-Rehel, J. J. Peron, A. Borgne, M. Walls and P. Guerin, *Polym. Degrad. Stab.* 2002, **76**, 411−417.
22 K.-Y. Chang, C.-C. Lin, G.-H. Ho, Y.-P. Huang and Y.-D. Lee, *Polymer* 2009, **50**, 1755–1763.
23 H. F. Liang, S. C. Chen, M. C. Chen, P. W. Lee, C. T. Chen and H. W. Sung, *Bioconjug. Chem.* 2006, **17**, 291.
24 R. E. Drumright, P. R. Gruber and D. E. Henton, *Adv. Mater.* 2000, **12**, 1841–1846.
25 F. Nederberg, E. F. Connor, M. Möller, T. Glauser and J. L. Hedrick, *Angew. Chem. Int. Ed.* 2001, **40**, 2712–2715.
26 a) Z. Zhao, Z. Zhang, L. Chen, Y. Cao, C. He and X. Chen, *Langmuir* 2013, **29**, 13072–13080. b) D. Pasini, P. P. Righetti and V. Rossi, *Org. Lett.* 2002, **4**, 23–26.
27 C. Zhou, H. Guo, J. Li, S. Huang, H. Li, Y. Meng, D. Yu, J. de Claville Christiansen and S. Jiang, *RSC Adv.* 2016, **6**, 113762.
28 J. A. Portilla-Arias, M. García-Alvarez, A. Martínez de Ilarduya and S. Muñoz-Guerra, *Polym. Deg. Stab.* 2007, **92**, 1916.
29 T. Kawai, N. Rahman, G. Matsuba, K. Nishida, T. Kanaya, M. Nakano, H. Okamoto, J. Kawada, A. Usuki, N. Honma, K.

Nakajima and M. Matsuda, *Macromolecules* 2007, **40**, 9463–9469.
30 M. Yasuniwa, K. Sakamo, Y. Ono and W. Kawahara, *Polymer* 2008, **49**, 1943–1951.
31 a) K. Wasanasuk and K. Tashiro, *Polymer* 2011, **52**, 6097–6109. b) H. Tsuji, K. Iguchi, K. Tashiro and Y. Arakawa, *Polym. Chem.* 2020, **11**, 5711–5724.
32 a) R. L. Atkinson, O. R. Monaghan, M. T. Elsmore, P. D. Topham, D. T. W. Toolan, M. J. Derry, V. Taresco, R. A. Stockman, D. S. A. De Focatiis, D. J. Irvine and S. M. Howdle, *Polym. Chem.* 10.1039/D1PY00326G. b) S. Y. Yu-Su, F. C. Sun, S. S. Sheiko, D. Konkolewicz, H. Lee and K. Matyjaszewski, *Macromolecules* 2011, **44**, 5928–5936. c) D. Wang and T. P. Russell, *Macromolecules* 2018, **51**, 3–24.
33 J. C. Stockert, R. W. Horobin, L. L. Colombo, A. Blázquez-Castro, *Acta Histochemica* 2018, **120**, 159–167.
34 T. Kean and M. Thanou, *Adv. Drug Deliv. Rev.* 2010, **62**, 3–11.
35 D. Dou, G. He, Y. Li, Z. Lai, L. Wei, K. R. Alliston, G. H. Lushington, D. M. Eichhorn and W. C. Groutas, *Bioorg. Med. Chem.* 2010, **18**, 1093–1102.
36 E. Harder, W. Damm, J. Maple, C. Wu, M. Reboul, J. Y. Xiang, L. Wang, D. Lupyan, M. K. Dahlgren, J. L. Knight, J. W. Kaus, D. S. Cerutti, G. Krilov, W. L. Jorgensen, R. Abel and R. A. Friesner, *J. Chem. Theory Comput.* 2016, **2**, 281–296.
37 W. C. Still, A. Tempczyk, R. C. Hawley and T. Hendrickson, *J. Am. Chem. Soc.* 1990, **112**, 6127–6129.
38 G. Chang, W. C. Guida and W. C. Still, *J. Am. Chem. Soc.* 1989, **111**, 4379–4386.
39 M. Saunders, K. N. Houk, Y.-D. Wu, C. W. Still, M. Lipton, G. Chang and W. C. Guida, *J. Am. Chem. Soc.* 1990, **112**, 1419.
40 E. Polak and G. Ribiere, *Revue Francaise Inf. Rech. Oper., Serie Rouge* 1969, **16-R1**, 35.
41 J.-P. Ryckaert, G. Ciccotti and H. J. C. Berendsen, *J. Comput. Phys.* 1977, **23**, 327.

**Table of Contents Graphics**

Biocompatible graft copolymers from bacterial poly(γ-glutamic acid) and poly(lactic acid) are realized using a "grafting to" approach combined with click chemistry.